Engineering Science and Technology, an International Journal 45 (2023) 101491

Contents lists available at ScienceDirect

Engineering Science and Technology, an International Journal

journal homepage: www.elsevier.com/locate/jestch

Sensor-based microwave brain imaging system (SMBIS): An experimental six-layered tissue based human head phantom model for brain tumor diagnosis using electromagnetic signals

Amran Hossain [a,b], Mohammad Tariqul Islam [a,*], Ahasanul Hoque [c], Sharul Kamal Abdul Rahim [d], Ahmed S. Alshammari [e], Muhammad E.H. Chowdhury [f], Mohamed S. Soliman [g,h]

[a] Centre for Advanced Electronic and Communication Engineering, Department of Electrical, Electronic and Systems Engineering, Faculty of Engineering and Built Environment, Universiti Kebangsaan Malaysia, 43600 Bangi, Malaysia
[b] Department of Computer Science and Engineering, Dhaka University of Engineering and Technology, Gazipur, Gazipur 1707, Bangladesh
[c] Institute of Climate Change (IPI), Universiti Kebangsaan Malaysia, 43600 Bangi, Malaysia
[d] Wireless Communication Centre, Universiti Teknologi Malaysia, 81310 Skudai, Malaysia
[e] Department of Electrical Engineering, College of Engineering, University of Ha'il, Ha'il 81481, Saudi Arabia
[f] Department of Electrical Engineering, Qatar University, Doha 2713, Qatar
[g] Department of Electrical Engineering, College of Engineering, Taif University, P.O. Box 11099, Taif 21944, Kingdom of Saudi Arabia
[h] Department of Electrical Engineering, Faculty of Energy Engineering, Aswan University, Aswan 81528, Egypt

ARTICLE INFO

Keywords:
Tissue mimicking head phantoms
Brain tissues
Brain tumor diagnosis
Stacked antenna sensor
Sensor-based microwave brain imaging system
Benign tumor
Malignant tumor

ABSTRACT

The paper presents the preparation and measurement of six-layered human head phantoms for the sensor-based microwave brain imaging system (SMBIS) for the diagnosis of tumors in the head. The head phantom has been constructed based upon three-dimensional arrangements filled-up with numerous biochemical combinations that imitate the six brain tissues: DURA, CSF, White Matter, Gray Matter, Fat, and Skin regarding permittivity within the wideband frequency band (1 GHz to 4 GHz). For imaging purposes, the malignant and benign tumor(s) are also fabricated and placed in different locations in the 3D skull model to validate the performance of the phantom. After being formulated, the dielectric properties are measured by utilizing a dielectric kit linked with a vector network analyzer. The measured dielectric properties are compared to real human head tissue's dielectric properties. After that, the human phantom model, including tumors, is validated using a SMBIS. The investigational dielectric characteristics of the brain tissues showed good agreement with the dielectric properties of the real brain tissues of the head. The experimental imaging outcomes demonstrated the legitimacy of the proposed six-layered tissue mimicking phantoms that can be used as an alternate to the actual human brain tissue for the diagnosis of brain tumors in SMBIS.

1. Introduction

At present, several imaging technologies, such as computed tomography (CT) scanning, magnetic resonance imaging (MRI), X-ray mammography, ultrasound, and positron emission tomography are used to detect brain abnormalities in the human head in the medical investigative system (MIS) [1]. However, due to lots of drawbacks of the stated technologies, for example, ionizing radioactivity, false-negative parentage, dangerous radiation, more expensive, and raising cancerous hazards, the scholars are inspired to develop an alternative technology to alleviate these complications. Over the last decade, microwave imaging (MWI) technology has been proposed to mitigate these problems and detect brain abnormalities due to its low cost, non-ionizing nature, lightweight, low profile, and portable characteristics [2–7]. However, for testing the validity and performance outcomes of the MWI technology, a live patient is needed, but this is not possible due to the life risk without a clinical trial [8]. Thus, before moving to a clinical trial on the human head, the alternate solution is to develop an artificial anatomical head phantom with layers that mimic a realistic head and must have the dielectric properties of the human head tissues

* Corresponding author.
E-mail address: tariqul@ukm.edu.my (M. Tariqul Islam).

https://doi.org/10.1016/j.jestch.2023.101491
Received 6 April 2023; Received in revised form 21 June 2023; Accepted 14 July 2023
Available online 3 August 2023

as close as possible. A human head consists of six layers, such as skin, skull, fat, CSF, gray matter, and white matter [2,5]. All layers have distinct dielectric properties (i.e., relative permittivity and conductivity), and they have different geometry distributions. As a result, the sophisticated anatomical geometry, resistivity, thickness, depth, and other mentioned properties of the tissues in the human head, there is a significant challenge to constructing an accurate head phantom for a microwave imaging system. Besides, choosing the exact ingredient materials is another issue for making the head tissues with their respective properties, which are mimicked as closely as realistic head tissues. Though the phantom is a numerical and physical model that signify the features of a few required human anatomical structures [9,10]. Phantoms are an economical approach to assessing various electromagnetic (EM) applications, especially numerous medical diagnostic imaging and microwave imaging applications. However, it is noticeable that the head phantoms are replicas of brain tissues or organs intended to mock the formation and physical assets of their biologically identical parts. The dielectric characteristics are the interesting parameters in the head. A human head has heterogeneous characteristics with distinct properties of the dielectric of the head tissues due to corresponding components like water, fat, and protein [11,12]. Considering the distinct properties of the head tissues, the researchers have been made different categories of head phantoms for imaging purposes. For instance, a heterogeneous phantom [13–15], anthropomorphic heterogeneous phantoms [16–18], 3D-printed phantom [19], four-shell diffusion phantom [20], a plaster phantom [21], reconfigurable phantom [22], head-sized phantom [23], synthetic MRI-based phantom [24].

A heterogeneous head phantom for quality control in stereotactic radiosurgery has been presented and discussed in [15]. The authors in [15] have fabricated only the head skull and brain tissue and investigated it for computed tomography imaging purposes. Polymethyl methacrylate and polytetrafluoroethylene are used as the main ingredients, which are comparatively high cost, and this phantom is not suitable for microwave imaging as well as they did not mention the measurement outcomes of the dielectric properties of the tissues. A realistic heterogeneous head phantom is fabricated and presented in [14] for microwave imaging purposes. In this fabrication process, the authors used polyvinyl chloride, agar, sodium azide, agar, and gelatin as the main ingredients, but they fabricated only three tissues and used a commercial skull for measurement. In [13], the authors have presented a heterogenous head phantom for microwave tomography imaging. The authors have used a plastic container as a skull and fabricated only brain tissue by using commercial ingredients. The gelatin, water, oil, carbon powder polyurethane, and graphite isopropanol are used for fabricating the brain tissues. However, the imaging result may be ambiguous due to the lack of dielectric characteristics in other tissues of the head phantom as well as the low measured dielectric properties are relative to the real tissue properties. An anthropomorphic head phantom's construction methodology has been illustrated in [17] for susceptibility artifacts of the head phantom. In this phantom fabrication, the authors used a plastic-based commercial skull for testing purposes as well as $MnCl_2$ solution, NaCl, WAX, and rubber bung as the main ingredients to fabricate brain tissues. However, the authors did not measure the dielectric features of the formulated tissues. Thus, the fabricated phantom is not appropriate for microwave imaging due to the lack of proper dielectric properties of the tissues. A 3D-printed structure-based anthropomorphic head phantom has been fabricated and presented in [16] for microwave imaging purposes. In this approach, the authors have made the brain, blood, and CSF tissues with the TX-100, salted water, graphite, carbon black, and silicon rubber and filled them into the skull. In [18], the authors have been presented the fabrication procedure of a realistic 3D anthropomorphic heterogeneous head phantom that has been tested for magnetic resonance imaging purposes. They used sodium chloride, distilled water, and ethanol solutions as the main ingredients to fabricate the head tissues, such as the brain, CSF, fat, and muscle, and filled them into the skull. However, they measured the dielectric properties at the frequency range from 295 MHz to 300 MHz, but this range is not appropriate for head imaging applications because the 1 GHz to 4 GHz range is needed for measuring microwave head imaging, as well as this fabrication is not suitable for microwave head imaging. A 3D-printed anatomical head phantom with skull resistivity distribution has been presented in [19] for electrical impedance tomography. They fabricated a 3D-printed skull, CSF, and printed brain tissues, and measured the complex resistivity distribution of the fabricated phantom, but they did not measure the actual dielectric properties of the tissues to validate the performance of the phantom. In [20], the authors have been constructed and presented a four-shell diffusion agar-based head phantom for electrical impedance tomography. In this fabrication, skull, CSF, and brain tissues have been fabricated to measure the resistivity of the skull, but the dielectric properties measurement outcome of the tissues was absent in this construction, and this phantom is not appropriate for microwave imaging applications due to the lack of dielectric properties in the frequency band. In [21], a 3D plaster head phantom has been fabricated and illustrated for computed tomography imaging. The authors have been fabricated only the skull and divided it into eight separate sections to measure the resistivity, but they did not measure the electrical features of the skull.

An anatomically and dielectrically reconfigurable head phantom has been presented in [22] for microwave imaging. The authors in [22] have been used graphite powder, a mixture of polyurethane rubber, and carbon powder as main ingredients to fabricate the skin, skull, CSF, and brain layers for measuring purposes, which are costly elements. They measured the dielectric properties of the tissues within the operating range of 0.5 GHz to 3.00 GHz, but the measured dielectric properties were comparatively low with respect to realistic tissues. A typical head-sized phantom has been presented in [23] for radiofrequency field characterization. The phantom was filled with a solution of polyvinylpyrrolidone that mimics brain tissue. However, the authors fabricated only one tissue, which is not appropriate to prove the characteristics of the head phantom as well as the measurement outcome of the tissue was disappeared in the paper. A synthetic MRI-based head phantom has been fabricated and presented in [24] for MRI imaging purposes. They fabricated only white matter, gray matter, and CSF tissues by using various concentrations of copper sulfate (97.5% purity) and normal saline, but there were no measured outcomes for the dielectric properties of head tissues [25,26]. As a result, it is not guaranteed that it will be suitable for microwave head imaging applications. It is observed that the stated fabricated phantom consists of four tissue layers and is utilized for microwave imaging purposes. But the major drawback of the system is, it creates noisy images with low detection accuracy. A head phantom has been fabricated for stroke detection and presented in [5]. In [5], the authors have been fabricated four tissue layers: gray matter, CSF, white matter, and DURA. The iteratively corrected CF-DMAS algorithm has been utilized to recreate images, but the reconstructed images were noisy due to time stability, and the detected object was very small. Thus, there is a demand for formulating six-layered tissues imitating brain phantoms that imitate real head properties with high resolution-based images and high detection accuracy. The key contributions of the research are as follows:

1. As per the knowledge of the authors, this is the first research work where a six-layered heterogeneous tissue imitating a head phantom is formulated that imitates real head tissues.
2. The fabricated tissues are measured and filled step by step in a 3D commercial human skull model, including benign and malignant tumor(s) for validating the imaging performances.
3. The fabricated head model is examined by employing a nine stacked-antenna sensor array based SMBIS to generate microwave brain tumor images to diagnose brain tumors.

The remaining part of the manuscript is structured as follows: Section 2 explains the sensitivity analysis of the simulated head model. The

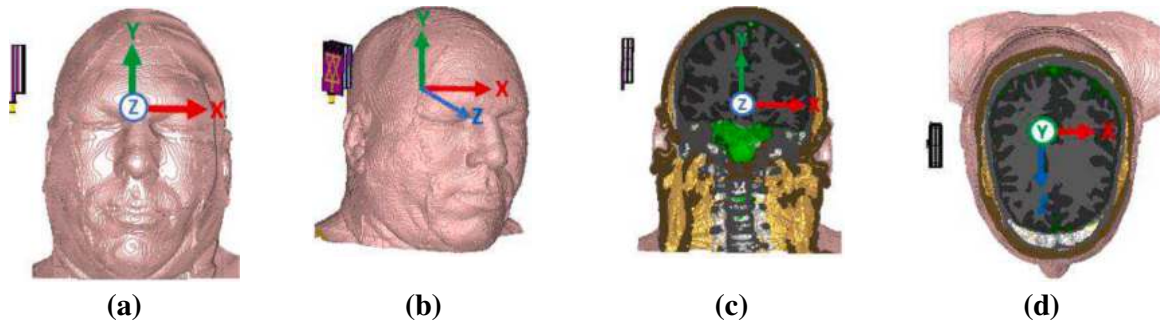

Fig. 1. Cross sectional view of Hugo model: (a) Face view; (b) Side view; (c) Coronal Plane; (d) Transverse plane.

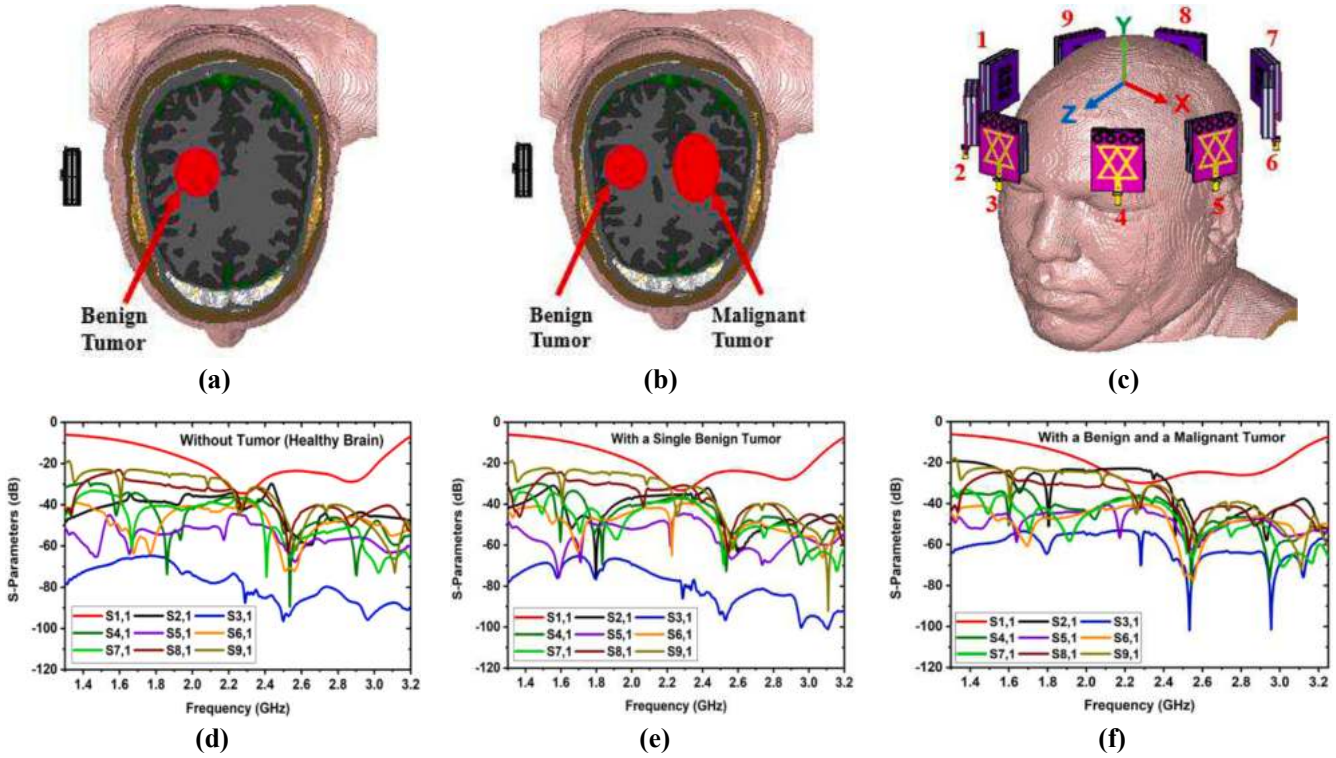

Fig. 2. Simulated environment with tumor location: (a) Location of the benign tumor in the model; (b) Locations of the benign (normal) and malignant (cancerous) tumor in the model; (c) Simulated environment with nine antenna sensor setups; (d) Reflected signals without tumor (i.e., healthy brain); (e) Reflected signals with a single benign tumor; (f) Reflected signals with a benign and a malignant tumor.

analysis of the simulated model using an antenna sensor is described in Section 2. Section 3 illustrates the brain phantom fabrication process. Phantom measurement processes and performance analysis are discussed in Section 4. Section 5 discusses the measurement outcomes of the fabricated phantom components. The imaging experiment and result analysis are illustrated in Section 6. In the end, the paper concludes in Section 7.

2. Sensitivity analysis of the simulated head model using antenna sensor

The sensitivity of a simulated phantom model by using single and nine stacked antenna sensors. Initially, we created a simulation framework using a Hugo head phantom model for performance analysis. The model is introduced from the CST (Computer Simulation Technology) (Version: 2019) software's voxel model. The Hugo model comprises seven tissue layers: Skull, DURA, CSF, White Matter, Gray Matter, Skin, and Fat. The tissues of the model imitate real human head tissues. The dielectric characteristics of tissues are the same as those of the real brain. So, before the fabrication of the model, it is essential to investigate the model's characteristics. The diverse and horizontal views of the model obtained by utilizing a single stacked antenna are depicted in Fig. 1.

The image reconstruction performance depends on the dielectric properties of the brain tissues. Thus, it is necessary to analyze the phantom characteristics with the presence of the abnormalities (i.e., tumors) in the human brain. Initially, we analyzed the healthy brain (i.e., without tumor) and unhealthy brain (i.e., with benign and malignant or cancerous tumors). So, a benign tumor and a malignant tumor are placed in the brain to analyze the performance. The locations of the tumors in the brain are presented in Fig. 2(a-b). Besides, a nine-stacked antenna array is set up surrounding the head model for investigating the performance of the Hugo model. The nine-antenna setup is presented in Fig. 2(c), where antenna 1 acts as a transmitter and the remaining eight antennas are used as receivers. The receiving antenna receives back-scattering signals. The simulated S-parameters for the normal brain, with a single benign tumor, and with a single benign tumor and a cancerous tumor in the brain are presented in Fig. 2(d-f) respectively. The operating band of 1 GHz to 4 GHz is considered during simulation.

Table 1
Required components for 500 g tissue formulation.

Ingredients/ Brain Tissues	Water (gm/ml)	Corn Flower (gm)	Gelatine (gm)	Agar (gm)	Sodium Azide (gm)	Propylene Glycol (gm)	Nacl (gm)	Sodium benzoate (gm)	N-Propanol (gm)
CSF	418.70	10.20	0.00	56.20	1.82	7.48	5.60	0.00	0.00
DURA	360.90	121.65	0.00	4.55	1.83	9.61	1.24	0.00	0.00
White matter	353.35	134.30	7.05	0.00	1.75	3.55	0.00	0.00	0.00
Gary matter	403.25	82.95	0.00	5.20	1.75	4.60	2.30	0.00	0.00
Malignant Tumor	404.85	15.55	….	63.55	1.30	5.28	6.42	1.55	1.25
Benign Tumor	409.84	13.36	…..	62.75	1.80	5.55	6.40	0.00	0.00

Table 2
Required components for 500 g skin and fat tissues formulation.

Ingredients	Water (gm/ml)	Corn Flower (gm)	Gelatine (gm)	Canola oil (gm)	Kerosene (gm)	Glycerin (gm)	Nacl (gm)	Sodium benzoate (gm)	N-Propanol (gm)	TX-151 (gm)
Tissues										
Skin	241.00	149.00	0.00	0.00	46.00	0.00	1.58	2.20	0.00	25
Fat	54.50	111.89	30	75.01	78.50	100	2.50	1.50	31.10	0.00

The stacked antenna operates within the band. The backscattered bio-signals for tumors are significantly distorted, as seen from the S-parameters. Due to the tumors' strong dielectric characteristics, these distortion discrepancies occurred.

3. Brain phantom fabrication process

In this work, a heterogeneous head phantom is fabricated. In general, a human head consists of seven tissue layers, such as skin, fat, skull, dura, CSF, gray matter, and white matter. The brain is made of a combination of two layers: gray and white matter. It is noted that every head tissue has distinct dielectric properties. Thus, selecting the ingredients as materials is a significant factor in fabricating the different tissues of the phantom with their respective dielectric properties, which are mimicked as the realistic characteristics of the phantom. In this work, we used a commercially available 3D blank skull and fabricated other tissues for experimental purposes, and this phantom is suitable for microwave head imaging applications. However, we have selected seven low-cost-based materials as prime ingredients, such as distilled water, corn flour, gelatine, agar, sodium chloride (NaCl), propylene glycol, sodium azide, sodium benzoate, N-propanol, glycerin, kerosene, and TX-151 [16,27]. The equivalent composition quantity of all ingredients used in making 500 gm of heterogeneous brain tissue of the head phantom is presented in Table 1 and Table 2. Distilled water is used to increase the dielectric values because it is a basis of permittivity and high dielectric values over a wideband. In this case, if tap water is used, the conductivity of the mixture may be increased. Corn flour is used to meet two purposes, one is to enhance the viscosity of the mixtures, and the other is to maintain the bonding between the different layers of the tissues. Gelatine is used as a thickener, and it has dielectric properties and is very close to the head tissues. It also helps to stabilize the phantom for a long time and control the relative permittivity. The agar is used to control the shape of the phantom as well as prevent the separation of the water content. The propylene glycol component is used in the mixture due to its low conductivity characteristics and stabilizing of the mixture agent. In addition, it is also used for preservation purposes because it lowers the

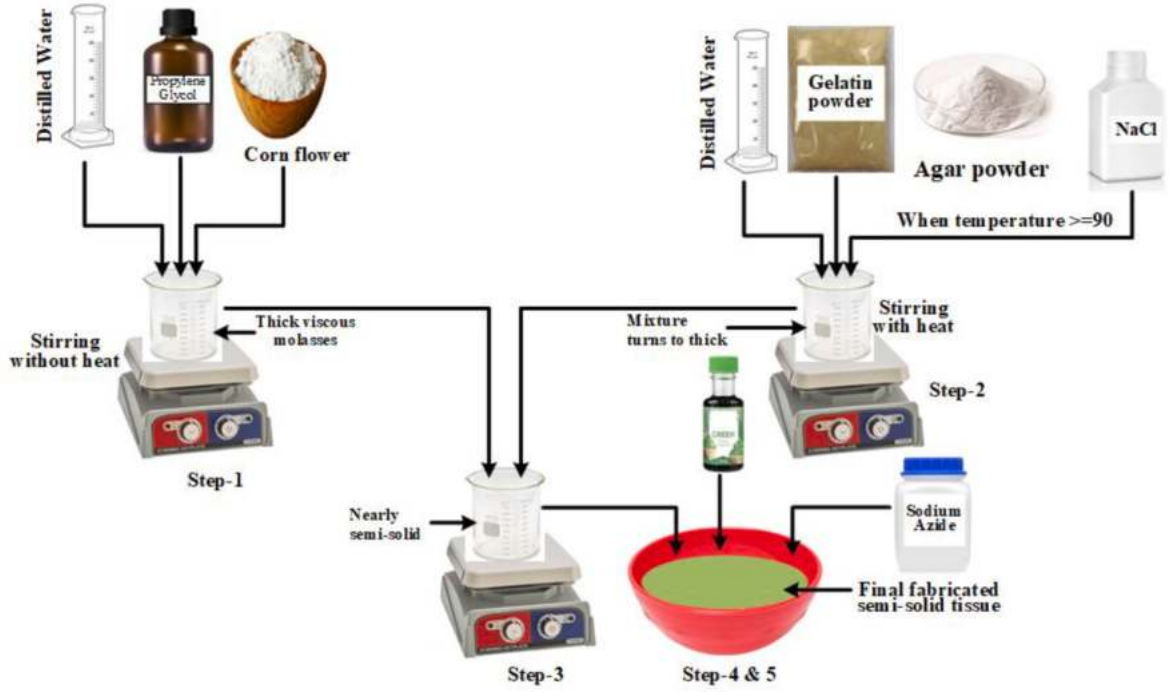

Fig. 3. Head phantom fabrication procedure.

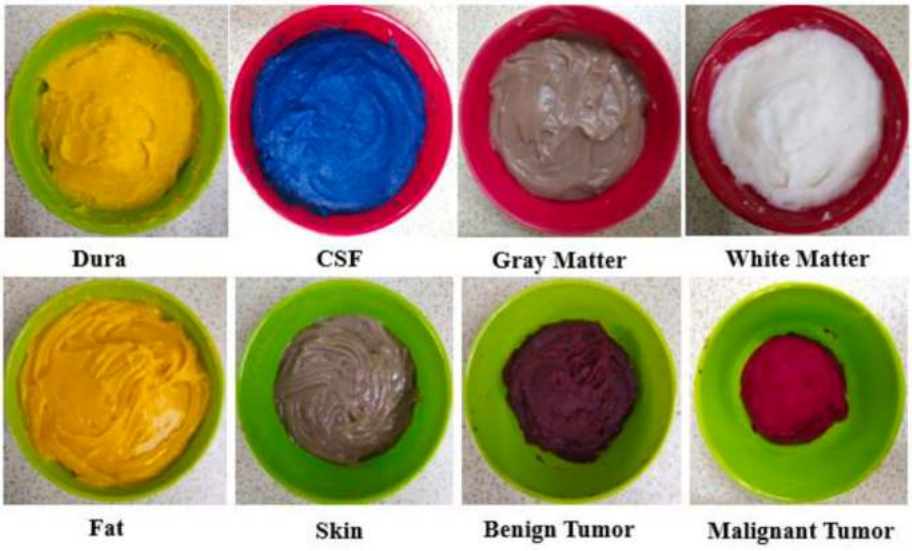

Fig. 4. Six fabricated phantoms including benign and malignant tumor.

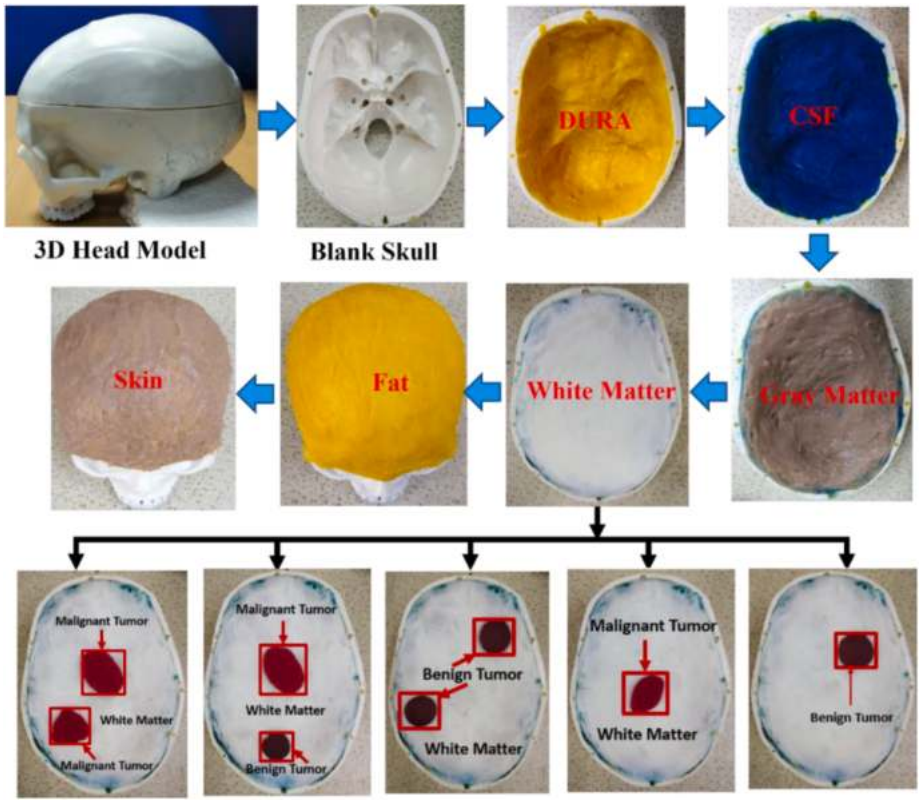

Fig. 5. Step-by-step phantom filling process in 3D skull including tumor placement.

freezing temperature of the fabricated tissues. Sodium azide is used in the mixtures as a preservative that controls conductivity. Also, NaCl is used in mixtures to improve and control the conductivity of the tissues.

Recently, microwave head imaging has become a popular technology in the biomedical research area, but human brain imaging is significantly more complex because of the complexity of the structural shape, functional properties, distinct electrical properties, and homogeneous characteristics of the human head tissues. Thus, it is a more challenging task to make a head phantom without changing the dielectric properties of the tissue layers. This research work only used a commercial 3D blank head skull and fabricated six layers: Skin, Fat, Gray Matter, White Matter, DURA, and CSF tissue layers. In addition, we also fabricated benign and malignant tumors. The fabrication process is visually presented in Fig. 3. The ingredients for the fabrication of the tissues are presented in Tables 1 and 2.

The overall tissue fabrication method is discussed step-by-step as follows:

Step-1: Firstly, at room temperature in a beaker, one-third of the distilled water is added with the propylene glycol and stirred gradually at 270 rpm by a magnetic hot plate without applying heat. Thereafter, the corn flour is mixed, and mixture is stirred gradually at 280 rpm until it forms a thick viscous molasses.

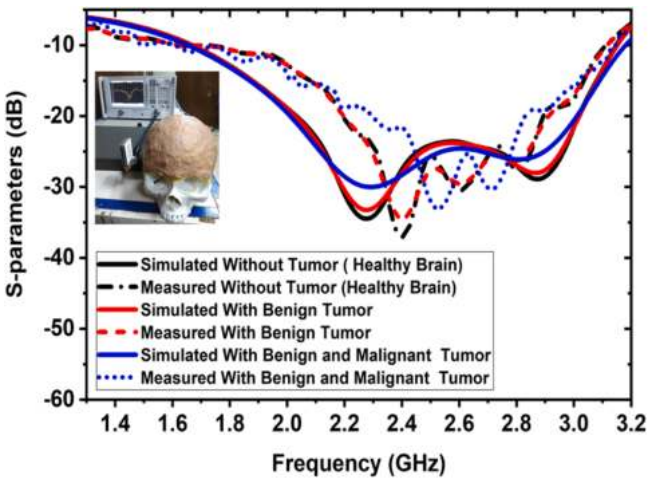

Fig. 6. Simulated and measured S-parameters with the fabricated head model.

Step-2: Besides, in another beaker, the ingredients gelatine or agar as mentioned in Table 2 are added with the remaining water, and stirred at 280 rpm, as well as gradually heated up to 90 $^{\circ}C$ to 95 $^{\circ}C$ by a magnetic hot plate. After raising the temperature, the NaCl is added to the mixture, and heating is continued for about 3 to 4 min until the gelatine or agar is melted. During the heating process, observe the bubble formation. In this case, it is noted that if fewer bubbles appear, it means the mixture turns thick, and if big bubbles are observed, it means the end of the stage.

Step-3: At the end of step 2, the previous viscous syrup of step 1 is added to the mixture of step 2, and heating continues with stirring until the mixture turns almost semi-solid**.**

Step-4: The heating gradually decreased and stopped after 2–3 min. In this scenario, the mixture is poured into another pot and allowed to cool down to 40 $^{\circ}C$ to 45 $^{\circ}C$ degrees and sodium azide is added to the mixture and stirred with a spoon until it forms the desired semi-solid.

Step-5: Finally, to differentiate the tissue layers in the head phantom, different food colors are added, mixed properly, and stored in semi-solid materials.

The fabricated six-layered tissues and benign and malignant tumors are portrayed in Fig. 4. In addition, Fig. 5 shows the process of inserting the phantom components one at a time into a 3D skull. The DURA component is added to it first, followed by CSF, Gray Matter, and White Matter, in that order. Then, for reasons of verification, the benign and malignant tumor(s) are placed in various locations. Next, the layers of fat and skin cover the skull, respectively. The head model tumor's area is indicated by a rectangle mark, and the iteratively corrected CF-DMAS algorithm [28] is then used to reconstruct the brain image and examine the phantom's performance.

4. Phantom measurement process and performance analysis

The experimental SMBIS will be used to explore a six (06) layered tissue-imitating phantom with various layers and tumor(s). The model's tumors are positioned in various locations. Fig. 6 displays the simulated and measured scattered signals (S-param.) of the constructed phantom without & with tumor utilizing an antenna sensor. With resonance frequencies, the reflection coefficients slightly decrease and shift towards higher frequencies. Fig. 6 shows that there is little variation between the outputs of simulation and measurement. The alteration of the brain layers and the dielectric characteristics of the tumor can result in this scenario. In this study, we used a computer simulation to create a realistic "Hugo head" model, complete with tumors, with set tissue thickness, as well as dielectric characteristics. However, due to

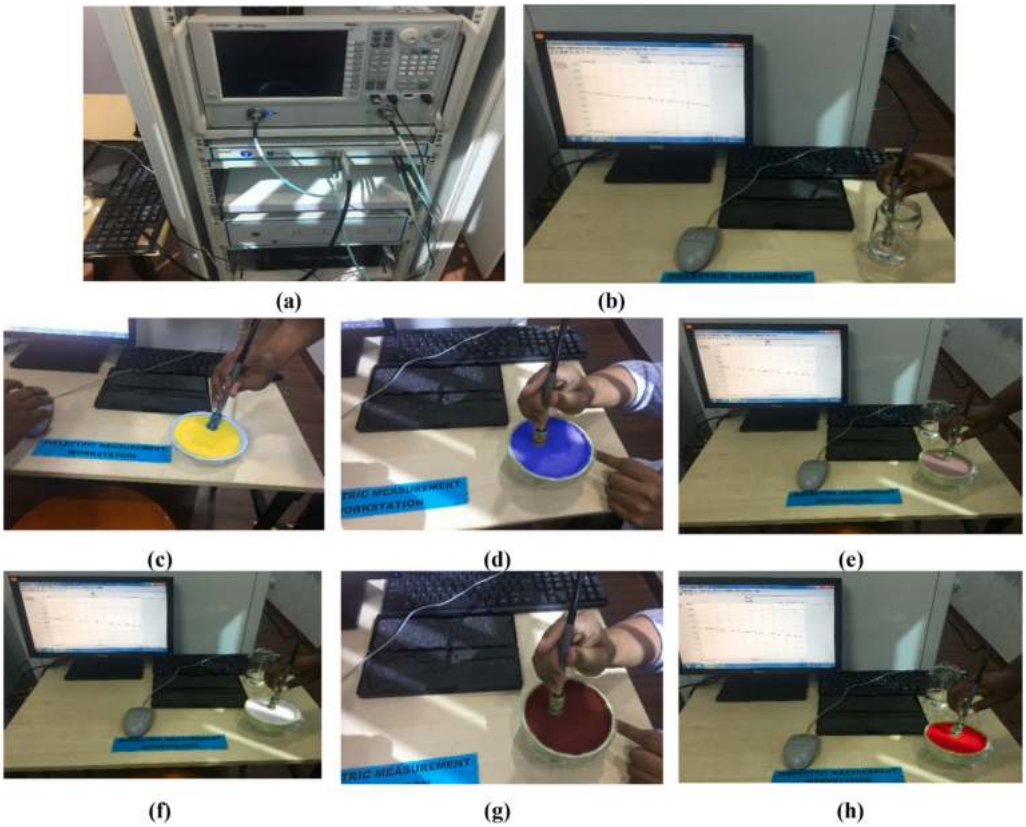

Fig. 7. The fabricated phantom measurement process and sample picture: (a) Experimental setup with PNA; (b) Sterile water calibration; (c) DUAR; (d) CSF; (e) Gray matter; (f) White matter; (g) Benign tumor; (h) Malignant tumor.

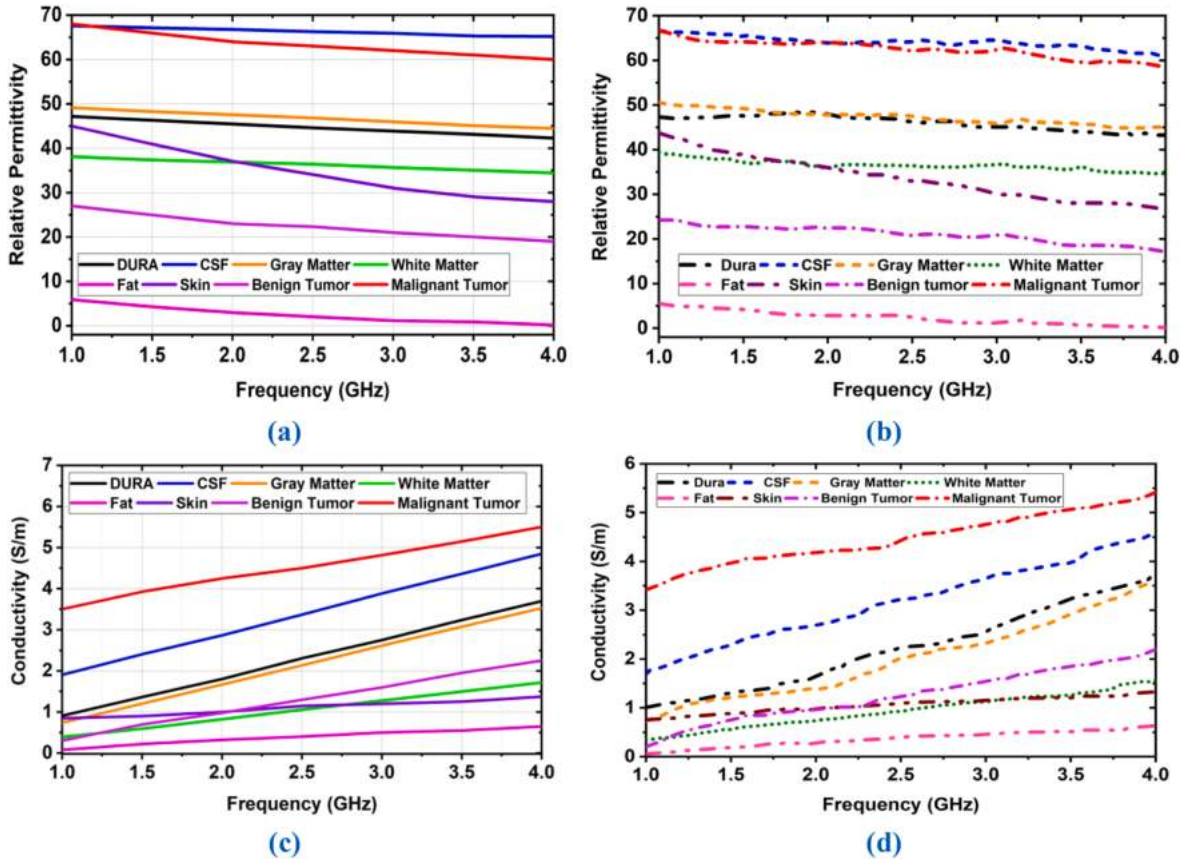

Fig. 8. Dielectric properties measurement of human brain tissues: (a) Standard reference of relative permittivity of six tissues and tumors (b) Measured relative permittivity of six tissues and tumors (c) Standard reference of conductivity of six tissues and tumors (d) Measured conductivity of six tissues.

fabrication tolerance, the formulated tissues' dielectric and thickness characteristics have changed fairly. (i.e., combination of ingredients and thickness).

Additionally, the results of measurements are impacted by free space measurement, environmental temperature, and temporal variation variables. The effectiveness of the stacked antenna array causes a discrepancy between the simulated and measured results, yet they both stay steady in the requisite operating band. However, the simulated and measured outcomes showed good agreement. For microwave head imaging, a wideband frequency range from 1 GHz to 4 GHz is needed. Thus, measurement of the dielectric properties of the head tissues must lie between 1 GHz and 4 GHz. So, the measurement is taken in a wideband frequency range (1 GHz to 4 GHz). A dielectric probe (KEYSIGHT technology, Model: 85070E) is used to measure the dielectric properties (Relative permittivity and Conductivity) and loss tangent (Tan δ), which is connected to a Vector Network Analyzer (Model: PNA-L N5232A, Operating Frequency: 300 KHz to 20 GHz).

The prob test is the most popular and easiest technique to measure the dielectric properties [181920]. The KEYSIGHT 85070E dielectric probe kit and a power network analyzer (PNA, Model: PNA-L N5232A; 300 KHz to 20 GHz) are used to measure the dielectric properties of the artificial tissues. The open-ended coaxial probe procedure is utilized to assess the electrical characteristics of the fabricated tissue-imitating head phantom. This method is straightforward, non-harmful, and useful for measurements over a broad frequency regime. Nevertheless, it is believed that there are limits to the accuracy of measurements due to the intricate and diverse constructions and irregular surfaces in homogeneous structures. Measurement processes and measuring equipment PNA are the key constraints for measuring contents. The humidity, pressure, temperature, and system modules, like the spotlessness of the probe tip, should be taken into account for an accurate reading. For the dielectric probe kit, the transmission line through which the bio-signals propagate in the coaxial cable is shut off. Exposed waves are caused by an impedance discrepancy between the probe and the desired tissue sample, which is later converted into complex permittivity values.

Fig. 7(a-b) portray the preliminary adjustment stage employing the VNA and coaxial cable (probe) with 25 cm^3 of sterilized water. After that, every sample of the phantom is divided independently to provide adequate contact between the sample (the formulated phantom) and the kit (the probe) during the measuring process. Later, the exterior of the phantom sample is shiny and flat to make sure that no space between the kit and sample element. A visible examination of the formulated sample is examined to confirm its consistency. In this experiment, the coaxial kit is randomly placed on the surface of the phantoms many times (4 times) for more precise data collection. Then, using the numerous data points that were gathered, the mean value of the assessment is determined. Fig. 7(c-h) show an example measurement setup image of the manufactured phantom components.

5. Dielectric properties measurement of the brain phantom components

The dielectric characteristics of the phantom are tested, and the relative permittivity and conductivity are compared with reference values. The dielectric properties of biological tissues in the human brain oversee the relations between the incident electromagnetic field and tissue components. The conductivity of brain tissues is a quantity of the thickness and movement of ions conveyed in the brain by an applied electric field. In contrast, the permittivity is the amount of the tissue's capability for the electric dipoles to reserve electric energy. In this work, the standard reference values of the dielectric properties of real human brain tissues in the frequency range of 1 GHz to 4 GHz are considered for

Table 3
Measured Relative permittivity and conductivity of the formulated brain phantoms at 2 GHz.

Fabricated Brain Tissues	Properties	Collected Data Samples From Four Locations				
		Sample 1	Sample 2	Sample 3	Sample 4	Mean
DURA	Relative Permittivity(ε_r)	45.01	44.05	41.52	43.63	43.55
	Conductivity (S/m)	2.45	2.25	1.87	2.15	2.18
CSF	Relative Permittivity(ε_r)	67.15	59.25	63.18	65.14	63.68
	Conductivity (S/m)	3.56	2.45	3.15	3.46	3.15
White Matter (WM)	Relative Permittivity(ε_r)	35.11	33.44	37.45	36.74	35.69
	Conductivity (S/m)	1.18	1.21	1.27	1.26	1.23
Gary Matter (GM)	Relative Permittivity(ε_r)	48.52	43.25	46.25	40.85	44.71
	Conductivity (S/m)	2.26	1.90	2.18	1.85	2.04
Skin	Relative Permittivity(ε_r)	42.56	38.58	36.98	40.68	39.70
	Conductivity (S/m)	0.95	0.91	0.90	0.92	0.92
Fat	Relative Permittivity(ε_r)	5.95	3.54	5.25	4.15	4.72
	Conductivity (S/m)	0.40	0.32	0.38	0.25	0.26
Benign Tumor	Relative Permittivity(ε_r)	24.95	24.24	24.05	24.36	24.40
	Conductivity (S/m)	0.59	0.35	0.25	0.36	0.38
Malignant Tumor	Relative Permittivity(ε_r)	67.95	66.12	66.45	65.12	66.41
	Conductivity (S/m)	4.45	4.15	3.75	3.52	3.96

Table 4
Comparison between dielectric properties of standard reference values of real human head and measured values of fabricated head phantom.

Human Head Tissues	Dielectric Properties	Frequency Range			
		1 GHz to 4 GHz		at 3 GHz	
		Reference Values [16,22,29]	Measured Values	Reference Values [16,22,29]	Measured Values (±2% to ± 7%)
Skin	Relative Permittivity(ε_r)	45–27	44–26	37.0	33.20 ± 2.31
	Conductivity (S/m)	0.9–1.4	0.8–1.4	1.34	1.20 ± 0.84
Fat	Relative Permittivity(ε_r)	6–3	6–2	4.22	3.51 ± 1.34
	Conductivity (S/m)	0.2–0.6	0.2–0.6	0.13	0.15 ± 0.05
DURA	Relative Permittivity(ε_r)	47–42	47–43	41.3	43.12 ± 3.08
	Conductivity (S/m)	0.9–3.6	1–3.6	2.11	2.35 ± 0.25
Gray Matter (GM)	Relative Permittivity(ε_r)	49–44	51–45	48.0	45.85 ± 2.15
	Conductivity (S/m)	0.7–3.5	0.7–3.6	2.22	2.45 ± 0.25
White Matter (WM)	Relative Permittivity(ε_r)	38–34	39–34	35.5	34.45 ± 2.73
	Conductivity (S/m)	0.4 –1.7	0.3–1.6	1.51	1.39 ± 0.11
CSF	Relative Permittivity(ε_r)	68–65	68–66	64.4	64.35 ± 1.32
	Conductivity (S/m)	1.9– 4.8	1.7–4.6	4.01	3.75 ± 0.33
Malignant Tumor	Relative Permittivity(ε_r)	69–60	69–58	67.10	62.56 ± 4.83
	Conductivity (S/m)	3.5–5.5	3.4–5.4	4.45	4.52 ± 0.38
Benign Tumor	Relative Permittivity(ε_r)	27–19	24–18	21.12	21.02 ± 1.33
	Conductivity (S/m)	0.3–2.2	0.3–2.3	1.35	1.45 ± 0.16

performance verification. The standard reference permittivity ranges from 45 to 27, 6–3, 47–42, 49–44, 38–34, 68–65, 69–60, and 27–19 for the Skin, Fat, DURA, Gray Matter, White matter, CSF, Malignant tumor, and Benign tumor, respectively [16,22,29]. Also, the aforementioned series of phantom components' standard conductivities range from (in S/m) 0.9–1.4, 0.2–0.6, 0.9–3.6, 0.7–3.5, 0.4 –1.7, 1.9– 4.8, 3.5–5.5, and 0.3–2.2, respectively [16,22,29]. For assessing the efficacy of the dielectric characteristics of the phantoms, the open-ended coaxial probe is positioned in four more arbitrary locations in the fabricated phantoms. The measured permittivity of the fabricated tissues such as Skin, Fat, DURA, Gray Matter, White matter, CSF, Malignant tumor, and Benign tumor ranges from 44 to 26, 6–2, 47–43, 51–45, 39–34, 68–66, 69–58, and 24–18, respectively. On the other hand, the measured conductivity ranges (in S/m) from 0.8 to 1.4, 0.2–0.6, 1–3.6, 0.7–3.6, 0.3–1.6, 1.7–4.6, 3.4–5.4, and 0.3–2.3, respectively, for Skin, Fat, DURA, Gray Matter, White Matter, CSF, Malignant tumor, and Benign tumor. Fig. 8 illustrates the reference and measured dielectric properties of the fabricated brain tissues, including benign and malignant tumors, in the frequency range of 1 GHz to 4 GHz. As seen from Fig. 8, the reference and measured dielectric values of fabricated tissues are slightly inconsistent due to the tissue fabrication tolerance (i.e., lack of proper ingredient mixing and environmental temperature). As a result, 2% to 7% of measured values with respect to reference values can be slightly increased or decreased, which is acceptable [16]. However, measured values exist within the range. The standard reference values and measured dielectric properties of the fabricated tissues are illustrated in Fig. 8.

Table 3 presents the measured lists of data samples and their means that were obtained by PNA, which were taken from four locations of phantom elements at a frequency of 2 GHz. It is observed that the measured values of permittivity and conductivity are slightly different. It can happen due to the lack of a little bit of water molecules and gaps between mixing ingredients at different locations of the phantom. But the reference and measured parameters are almost identical. In order to assess the performance of the electromagnetic sensor-based microwave brain imaging system (SMBIS), the calculated phantom exhibits more realistic properties than the actual human brain tissues. The comparison of standard dielectric reference values of real human brain tissues and measured fabricated brain tissues is stated in Table 4. It is stated from Table 4 that the measured permittivity and conductivity of formulated brain tissues are slightly increased or decreased (±2% to ± 7%) because of fabrication tolerance, but still show outcomes within the range.

However, the used algorithm (i.e., IC-CF-DMAS) supports the tolerance of the deviation between CSF and malignant tumor since the delay parameter in the original DMAS calculated the travel time between source and detector (i.e., tumor object). While scattering signals penetrate through the proposed phantom of the system, they incorporate the background medium air and all phantom dielectric layers like CSF and

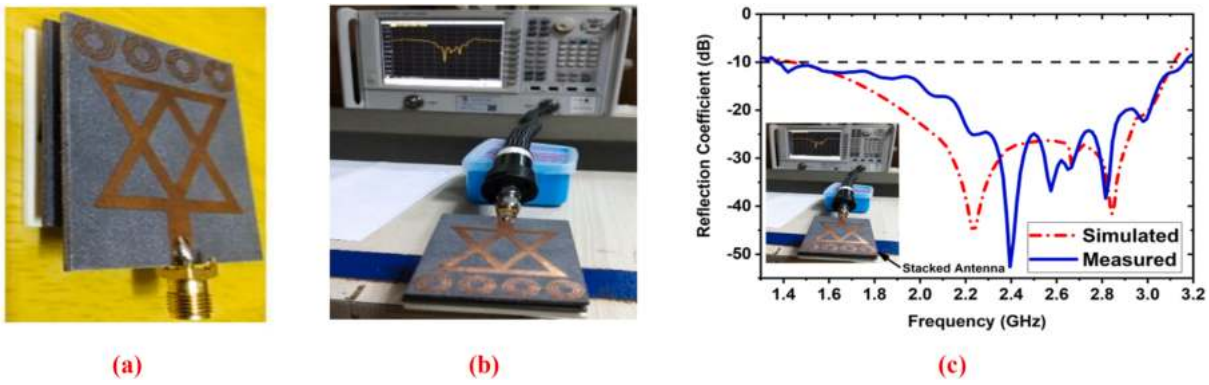

Fig. 9. A) Fabricated 3d sensor antenna (b) measurement process (c) reflection coefficient (scattering parameters).

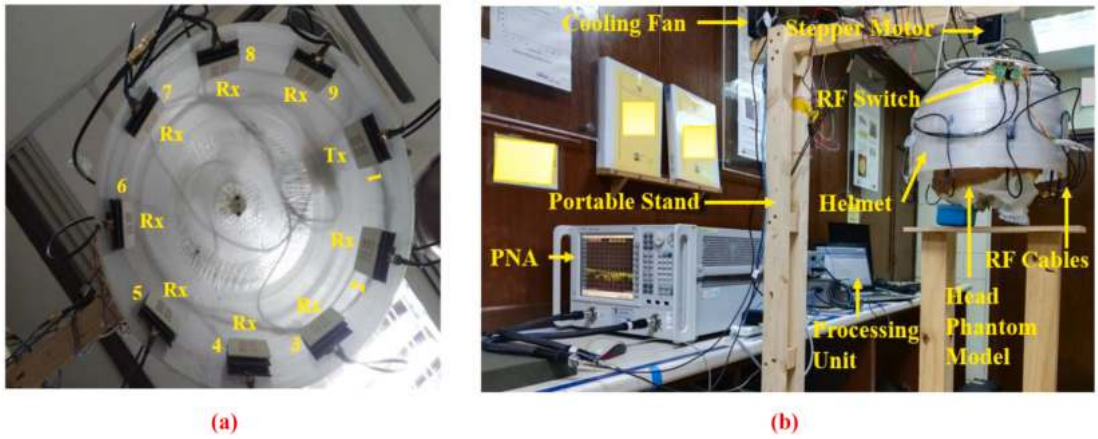

Fig. 10. Experimental SMBIS using six-layered head phantom: (a) Nine sensor-based antenna array setup inside the helmet; (b) Developed SMBIS.

malignant tumors. Furthermore, conductivity deviation and scattering parameters identified through algorithms define the specific values of CSF and malignant tumors for a particular frequency value. Hence, this delay parameter has encountered a slight deviation, which is depicted through simulated and measured dielectric properties characterization. So, based on this characterization by the algorithm, the antenna system could differentiate the CSF and malignant tumors.

6. Imaging experiment and result discussion

The fabricated phantom is evaluated by an investigational sensor-based MBI system (SMBIS). The SMBIS consists of a portable stand, a sensor-based stacked nine antenna arrays, a customized elliptical-shaped helmet, a stepper motor, a microcontroller, the PNA E8358A transceivers, and a switching circuit (RF switch). The 3D stacked antenna's overall dimension is $50 \times 40 \times 8.67$ mm^3. Initially, every single antenna is calibrated by a PNA calibration Kit and then scattering parameters are measured by the PNA to observe the antenna's performance. The 3D stacked antenna schematic diagram and measured outcomes (i.e., S-parameters) are depicted in Fig. 9. The nine antennas are set up in the interior of the helmet of the system, as shown in Fig. 10 (a). After setting up, the nine antennas in the system are calibrated by the PNA and switching matrix using the MATLAB system calibration program. This process is called the "blank data calibration process" that assists in observing the imaging performance. Fig. 10(b) shows the experimental MBI system. The portable platform, which is powered by a stepper motor, rotates 360 degrees around at a speed of 7.2 degrees per step. The customized helmet is designed using a Computer Aided Design (CAD) software. Then, the PETG (Polyethylene terephthalate glycol-modified) material is used to fabricate the helmet. The 3D printing machine is utilized to fabricate the helmet. The customized helmet is connected to the stepper motor and a motor shaft. The width of the customized helmet is 250 mm. With the help of two-sided lather tape, the sensor is placed interior the helmet. Each antenna must be spaced apart by a 40 degrees angle in order to cover the complete system. To change the position of the phantom head, the sensor is placed one hundred (100) millimeters up from the end of the helmet. The PNA relates to the computer throughout GPIB port A. In order to receive the backscattered signals, Port B is coupled to an radio frequency switching matrix and connected to the transmitting antenna.

A six-layered 3D head phantom model is built and positioned in the center of the helmet in order to test the system's efficacy. In a constructed head model, benign and malignant tumor(s) of various forms are placed to examine the imaging results. Additionally, the PNA collects the system's backscattered waves (S_{21}, S_{31},……. S_{91}) following every 7.2 degrees rotations. Thereafter, the IC-CF-DMAS image reconstruction algorithm [28] is utilized for the post-processing of the collected data to reconstruct the images of the brain tumors. The innovations of the used algorithm are (i) Algorithm can create multiple tumor-based image samples, (ii) It can provide images that are noise-free and clearly localize tumor objects in reconstructed images, and (iii) Reconstructing brain images require less computing time.

Fig. 11 represents the reconstructed brain images with and without tumor samples. Fig. 11(a-f) illustrated the non-tumor (NT), one benign tumor (OBT), one malignant tumor (OMT), two benign tumors (TBT), one malignant and one benign tumor (OMOBT), and two malignant tumor (TMT) image samples, respectively. It was found that the regional head area of the reconstructed images showed relatively low noise. The implemented SMBIS generated brain image samples with target tumors and their locations by utilizing formulated brain tissues.

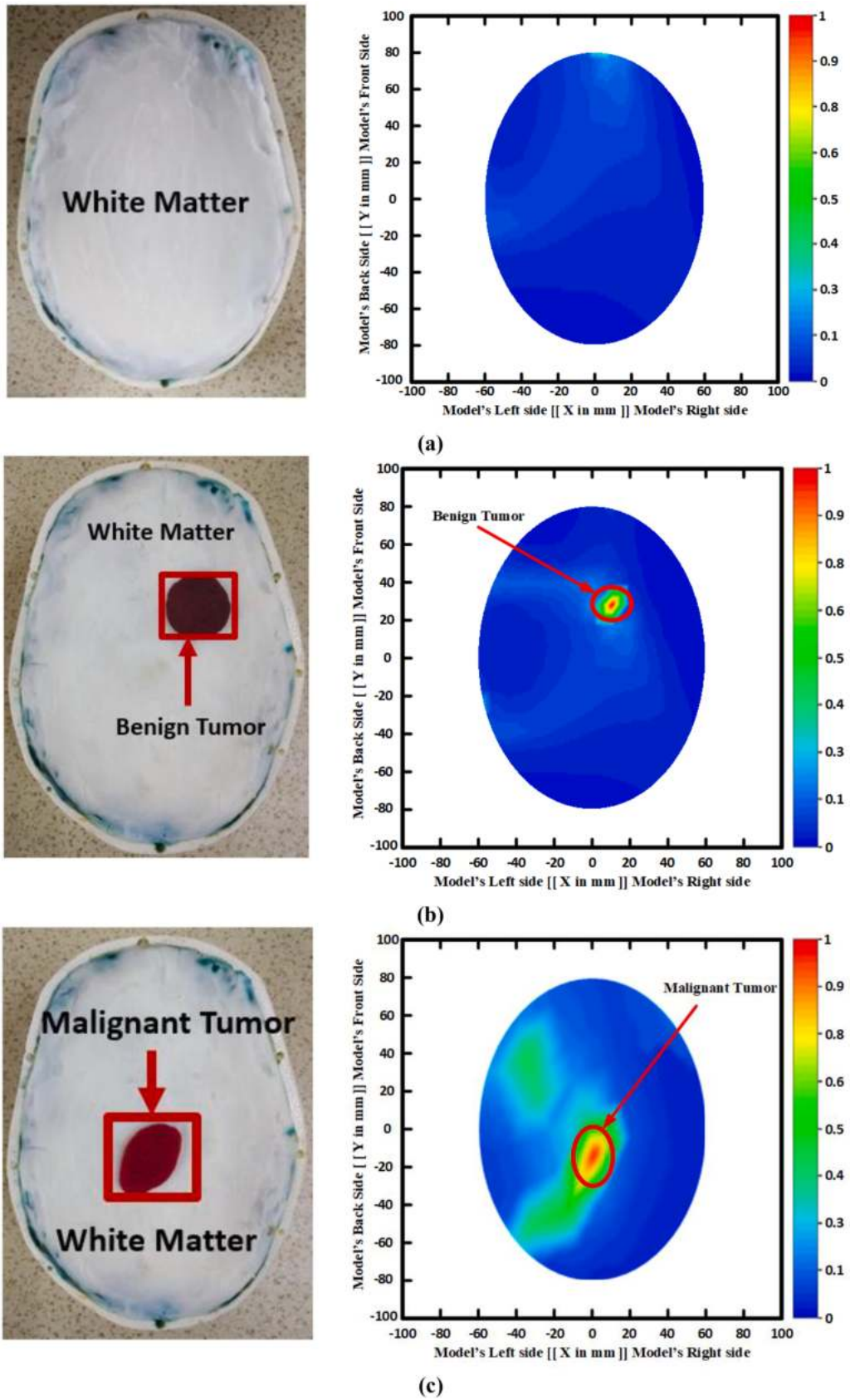

Fig. 11. Reconstructed brain images (a) Non-tumor (NT) (b) Single benign tumor (SBT) (c) Single malignant tumor (SMT) (d) Two benign tumors (TBT) (e) Single benign and single malignant tumor (SBSMT) (f) Two malignant tumors (TMT).

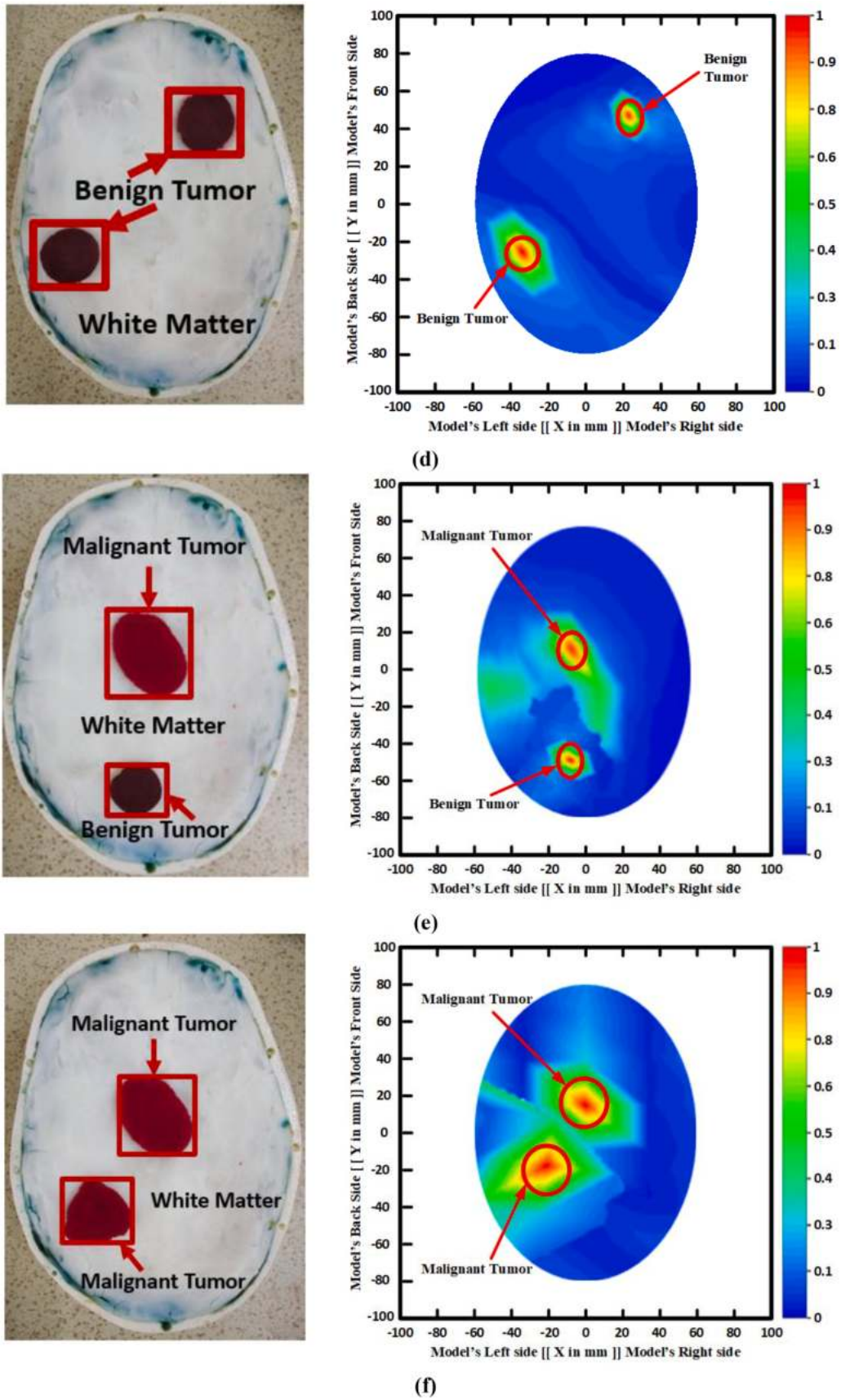

Fig. 11. (*continued*).

Table 5
Results of the proposed phantom model's comparison with established models.

Ref.	Frequency Range(GHz)	Type of Phantom	Fabricated Tissues	Structure	Algorithm for Image Reconstruction	DetectionResults	Application
[5]	1–4	Semi-solid heterogeneous	CSF, WM, GM, and DURA	Anthropomorphic	Iteratively corrected CF-DMAS	Single object	Microwave stroke imaging
[13]	0.5–2.5	Liquid,homogeneous	Only brain tissue	Anthropomorphic	DBIM-TwIST	One tumor with a Noisy image	Microwave tomography imaging
[14]	1–4	Semi-solid heterogeneous	CSF, WM, and GM	Anthropomorphic	Not stated	Not stated	Microwave brain imaging
[16]	1–6	Solid, acrylonitrile butadiene styrene (ABS)	WM, GM, and CSF	3D Anthropomorphic	Not stated	Not stated	Microwave brain imaging
[18]	0.29–0.3	Liquid, heterogeneous	Fat, CSF Brain, and Muscle	3D anthropomorphic	Segmentation slice based	One tumor with a Noisy image	Magnetic resonance imaging, and Electromagnetic imaging
[19]	Not stated	Solid, acrylonitrile butadiene styrene (ABS)	Skull, Brain, and CSF	3D printed anatomically	EIT based	One tumor with the blurry images	Microwave tomography imaging (MTI)
[22]	0.5–3.0	Semi-solid heterogeneous	Scalp, Skull, and CSF	Reconfigurable	Not stated	Not stated	Microwave brain imaging
[24]	Not stated	Liquid, heterogeneous	WM, CSF, and GM	synthetic MRI-based	Not stated	Only one Tumor	MBI System
Proposed	1–4	Semi-solid heterogeneous	Skin, Fat, DURA, CSF, WM, and GM	Anthropomorphic (tissue-mimicking)	IC-CF-DMAS	Double tumors with the high resolution images	SMBIS (Sensor-based Microwave brain imaging system)

The location and detection of the tumor(s) are shown in the images by the circular red mark. For identifying the tumor's location as a cartesian coordinate, both axis (left and bottom side) labels are used. Eight different tumor location(s) in the fabricated phantom model are considered in this research to investigate and assess the performance of the six-layered phantom model. It is concluded that the implemented head phantom can be used as a supplement to examine the tumor in SMBIS and can detect and locate the tumor(s) inside the brain. Table 5 compares the results of the proposed phantom model with established phantom models.

7. Conclusion

This article describes how a set of human head phantoms were prepared and measured for use with a SMBIS to find tumors. The head phantom was created using 3D structures filled with various chemical combinations that mimic the six types of brain tissue. For validating the performance of the phantom, the benign and malignant tumor(s) are also created and positioned in various locations for imaging explanations. Using a dielectric probe kit attached to a VNA, the dielectric properties are assessed after fabrication. The measured dielectric characteristics are contrasted with those of actual human skull tissue. After that, a 3D stacked wideband antenna-based microwave brain imaging system is used to validate the human phantom model with malignancies. The experimental dielectric properties of the brain tissues show good agreement with the standard reference dielectric properties of the real brain tissues of the head. The experimental imaging results depicted the validity of our proposed six-layered tissue-mimicking phantoms to be used in examination as a supplement to the real human brain tissue with two tumors and a comparatively high-resolution image.

Declaration of Competing Interest

The authors declare that they have no known competing financial interests or personal relationships that could have appeared to influence the work reported in this paper.

Acknowledgement

This research work was funded by the Ministry of Higher Education (MOHE), Malaysia through Fundamental Research Grants Scheme (FRGS) under the grant number: FRGS/1/2022/TK07/UKM/02/23.

References

[1] K. Kerlikowske, C.C. Gard, B.L. Sprague, J.A. Tice, D.L. Miglioretti, B.C. S. Consortium, One versus two breast density measures to predict 5-and 10-year breast cancer riskbreast density measures to predict breast cancer risk, Cancer Epidemiol. Biomarkers Prevent. 24 (2015) 889–897.
[2] A. Hossain, M.T. Islam, G.K. Beng, S.B.A. Kashem, M.S. Soliman, N. Misran, et al., Microwave brain imaging system to detect brain tumor using metamaterial loaded stacked antenna array, Sci. Rep. 12 (2022) 1–27.
[3] A. Hossain, M.T. Islam, M.E. Chowdhury, M. Samsuzzaman, A grounded coplanar waveguide-based slotted inverted delta-shaped wideband antenna for microwave head imaging, IEEE Access 8 (2020) 185698–185724.
[4] A. Hossain, M.T. Islam, M.T. Islam, M.E. Chowdhury, H. Rmili, M. Samsuzzaman, A planar ultrawideband patch antenna array for microwave breast tumor detection, Materials 13 (2020) 4918.
[5] M.S. Islam, M.T. Islam, A. Hoque, M.T. Islam, N. Amin, M.E. Chowdhury, A portable electromagnetic head imaging system using metamaterial loaded compact directional 3D antenna, IEEE Access 9 (2021) 50893–50906.
[6] A.T. Mobashsher, K.S. Bialkowski, A.M. Abbosh, S. Crozier, X. Zhang, Design and experimental evaluation of a non-invasive microwave head imaging system for intracranial haemorrhage detection, PLoS One 11 (4) (2016) e0152351.
[7] A.E. Stancombe, K.S. Bialkowski, A.M. Abbosh, Portable microwave head imaging system using software-defined radio and switching network, IEEE J. Electromagnet. RF Microwaves Med. Biol. 3 (4) (2019) 284–291.
[8] A. Salleh, C. Chiou Yang, T. Alam, M.S. Jit Singh, M.d. Samsuzzaman, M.T. Islam, Development of microwave brain stroke imaging system using multiple antipodal vivaldi antennas based on raspberry Pi technology, J. Kejuruterran 32 (1) (2020) 39–49.
[9] M. Caon, Voxel-based computational models of real human anatomy: a review, Radiat. Environ. Biophys. 42 (4) (2004) 229–235.
[10] C.-C. Chen, Y.-L. Wan, Y.-Y. Wai, H.-L. Liu, Quality assurance of clinical MRI scanners using ACR MRI phantom: preliminary results, J. Digit. Imaging 17 (4) (2004) 279–284.
[11] M.T. Islam, M.d. Samsuzzaman, M.T. Islam, S. Kibria, M.J. Singh, A homogeneous breast phantom measurement system with an improved modified microwave imaging antenna sensor, Sensors 18 (9) (2018) 2962.
[12] H. Woodard, D. White, The composition of body tissues, Br. J. Radiol. 59 (1986) 1209–1218.
[13] O. Karadima, M. Rahman, I. Sotiriou, N. Ghavami, P. Lu, S. Ahsan, P. Kosmas, Experimental validation of microwave tomography with the DBIM-TwIST algorithm for brain stroke detection and classification, Sensors 20 (3) (2020) 840.
[14] B.J. Mohammed, A.M. Abbosh, Realistic head phantom to test microwave systems for brain imaging, Microw. Opt. Technol. Lett. 56 (4) (2014) 979–982.
[15] M. Najafi, J. Teimouri, A. Shirazi, G. Geraily, M. Esfahani, M. Shafaei, Construction of heterogeneous head phantom for quality control in stereotactic radiosurgery, Med. Phys. 44 (2017) 5070–5074.
[16] N. Joachimowicz, B. Duchêne, C. Conessa, O. Meyer, Anthropomorphic breast and head phantoms for microwave imaging, Diagnostics 8 (2018) 85.

[17] K. Shmueli, D.L. Thomas, R.J. Ordidge, Design, construction and evaluation of an anthropomorphic head phantom with realistic susceptibility artifacts, J. Magnet. Reson. Imag. Off. J. Internat. Soc. Magnet. Reson. Med. 26 (1) (2007) 202–207.
[18] S. Wood, N. Krishnamurthy, T. Santini, S. Raval, N. Farhat, J.A. Holmes, T. S. Ibrahim, P. Lundberg, Design and fabrication of a realistic anthropomorphic heterogeneous head phantom for MR purposes, PLoS One 12 (8) (2017) e0183168.
[19] J. Zhang, B. Yang, H. Li, F. Fu, X. Shi, X. Dong, et al., A novel 3D-printed head phantom with anatomically realistic geometry and continuously varying skull resistivity distribution for electrical impedance tomography, Sci. Rep. 7 (2017) 1–9.
[20] A.D. Liston, R.H. Bayford, D.S. Holder, The effect of layers in imaging brain function using electrical impedance tomograghy, Physiol. Meas. 25 (1) (2004) 143–158.
[21] J.-B. Li, M.-X. Tang, X.-Z. Dong, C. Tang, M. Dai, G. Liu, X.-T. Shi, B. Yang, C.-H. Xu, F. Fu, F.-S. You, A new head phantom with realistic shape and spatially varying skull resistivity distribution, IEEE Trans. Biomed. Eng. 61 (2) (2014) 254–263.
[22] T. Pokorny, D. Vrba, J. Tesarik, D.B. Rodrigues, J. Vrba, Anatomically and dielectrically realistic 2.5 D 5-layer reconfigurable head phantom for testing microwave stroke detection and classification, Internat. J. Antenn. Propag. 2019 (2019) 1–7.
[23] W.M. Brink, Z. Wu, A.G. Webb, A simple head-sized phantom for realistic static and radiofrequency characterization at high fields, Magn. Reson. Med. 80 (2018) 1738–1745.
[24] C.-W. Li, A.-L. Hsu, C.-W. Huang, S.-H. Yang, C.-Y. Lin, C.-C. Shieh, W.P. Chan, Reliability of synthetic brain MRI for assessment of ischemic stroke with phantom validation of a relaxation time determination method, J. Clin. Med. 9 (6) (2020) 1857.
[25] N. Piladaeng, N. Angkawisittpan, S. Homwuttiwong, Determination of relationship between dielectric properties, compressive strength, and age of concrete with rice husk ash using planar coaxial probe, Measur. Sci. Rev. 16 (2016) 14.
[26] S. Seewattanapon, P. Akkaraekthalin, A broadband complex permittivity probe using stepped coaxial line, J. Electromagn. Anal. Appl. 03 (08) (2011) 312–318.
[27] A. Mobashsher, A. Abbosh, Three-dimensional human head phantom with realistic electrical properties and anatomy, IEEE Antenn. Wirel. Propag. Lett. 13 (2014) 1401–1404.
[28] M.S. Islam, M.T. Islam, A.F. Almutairi, A portable non-invasive microwave based head imaging system using compact metamaterial loaded 3D unidirectional antenna for stroke detection, Sci. Rep. 12 (2022) 1–27.
[29] C. Gabriel, Compilation of the Dielectric Properties of Body Tissues at RF and Microwave Frequencies, King's Coll London (United Kingdom) Dept of Physics, 1996.